JACC: CARDIOVASCULAR IMAGING VOL. ■, NO. ■, 2020

PUBLISHED BY ELSEVIER

ORIGINAL RESEARCH

[18F]-Florbetaben PET/CT for Differential Diagnosis Among Cardiac Immunoglobulin Light Chain, Transthyretin Amyloidosis, and Mimicking Conditions

Dario Genovesi, MD,[a,*] Giuseppe Vergaro, MD, PhD,[b,c,*] Assuero Giorgetti, MD,[a,*] Paolo Marzullo, MD,[a] Michele Scipioni, EngD,[d] Maria Filomena Santarelli, EngD,[e] Angela Pucci, MD,[f] Gabriele Buda, MD,[g] Elisabetta Volpi, BSc, PhD,[h] Michele Emdin, MD, PhD[b,c]

ABSTRACT

OBJECTIVES This study aimed to test the diagnostic value of fludeoxyglucose F 18 ([18F])-florbetaben positron emission tomography (PET) in patients with suspicion of CA.

BACKGROUND Diagnosis of cardiac involvement in immunoglobulin light-chain–derived amyloidosis (AL) and transthyretin-related amyloidosis (ATTR), which holds major importance in risk stratification and decision making, is frequently delayed. Furthermore, although diphosphonate radiotracers allow a noninvasive diagnosis of ATTR, demonstration of cardiac amyloidosis (CA) in AL may require endomyocardial biopsy.

METHODS Forty patients with biopsy-proven diagnoses of CA (20 ALs, 20 ATTRs) and 20 patients referred with the initial clinical suspicion and later diagnosed with non-CA pathology underwent a cardiac PET/computed tomography scan with a 60-min dynamic [18F]-florbetaben PET acquisition, and 4 10-min static scans at 5, 30, 50, and 110 min after radiotracer injection.

RESULTS Visual qualitative assessment showed intense early cardiac uptake in all subsets. Patients with AL displayed a high, persistent cardiac uptake in all the static scans, whereas patients with ATTR and those with non-CA showed an uptake decrease soon after the early scan. Semiquantitative assessment demonstrated higher mean standardized uptake value (SUV_{mean}) in patients with AL, sustained over the whole acquisition period (early SUV_{mean}: 5.55; interquartile range [IQR]: 4.00 to 7.43; vs. delayed SUV_{mean}: 3.50; IQR: 2.32 to 6.10; $p = NS$) compared with in patients with ATTR (early SUV_{mean}: 2.55; IQR: 1.80 to 2.97; vs. delayed SUV_{mean}: 1.25; IQR: 0.90 to 1.60; $p < 0.001$) and in patients with non-CA (early SUV_{mean}: 3.50; IQR: 1.60 to 3.37; vs. delayed SUV_{mean}: 1.40; IQR: 1.20 to 1.60; $p < 0.001$). Similar results were found comparing heart-to-background ratio and molecular volume.

CONCLUSIONS Delayed [18F]-florbetaben cardiac uptake may discriminate CA due to AL from either ATTR or other mimicking conditions. [18F]-florbetaben PET/computed tomography may represent a promising noninvasive tool for the diagnosis of AL amyloidosis, which is still often challenging and delayed. (A Prospective Triple-Arm, Monocentric, Phase-II Explorative Study on Evaluation of Diagnostic Efficacy of the PET Tracer [18F]-Florbetaben [Neuraceq] in Patients With Cardiac Amyloidosis [FLORAMICAR2]; EudraCT number: 2017-001660-38) (J Am Coll Cardiol Img 2020;■:■–■)

From the [a]Division of Nuclear Medicine, Fondazione Toscana Gabriele Monasterio, Pisa, Italy; [b]Division of Cardiology and Cardiovascular Medicine, Fondazione Toscana Gabriele Monasterio, Pisa, Italy; [c]Institute of Life Science, Scuola Sant'Anna Pisa, Pisa, Italy; [d]Information Engineering Department, University of Pisa, Pisa, Italy; [e]Consiglio Nazionale delle Ricerche, Institute of Clinical Physiology, Pisa, Italy; [f]Histopathology Department Pisa, University Hospital, Pisa, Italy; [g]Department of Clinical and Experimental Medicine, University of Pisa, Italy; and [h]Hospital Pharmacy, Fondazione Toscana Gabriele Monasterio, Massa, Italy. *Drs. Genovesi, Vergaro, and Giorgetti contributed equally to this work. The authors have reported that they have no relationships relevant to the contents of this paper to disclose.

ISSN 1936-878X/$36.00 https://doi.org/10.1016/j.jcmg.2020.05.031

ABBREVIATIONS AND ACRONYMS

AL = immunoglobulin light-chain–derived amyloidosis

ATTR = transthyretin-related amyloidosis

CA = cardiac amyloidosis

CI = confidence interval

CT = computed tomography

[18F] = fludeoxyglucose F 18

H/Bkg = heart-to-background uptake ratio

IQR = interquartile range

MV = molecular volume

PET = positron emission tomography

RI = retention index

SUV = standardized uptake value

TAC = time-activity curve

VOI = volumetric region of interest

Amyloidoses are a group of systemic inherited or acquired disorders characterized by extracellular deposition of amyloid insoluble fibrils, deriving from proteins encoded by mutated genes or from the misfolding of a normal protein (1). Cardiac involvement in amyloidosis is a major determinant of clinical presentation and may be present in primary immunoglobulin light-chain–derived amyloidosis (AL) and transthyretin-related amyloidosis (ATTR), either due to misfolded wild-type TTR (previously defined senile systemic amyloidosis) or to mutated TTR (also called variant) (2,3). Cardiac amyloidosis (CA) has an ominous prognosis that frequently is worse after a delay in diagnosis and treatment (4–7). Indeed, whereas ATTR has a recognized, specific, and sensitive diagnostic tool in diphosphonate scintigraphy, no imaging approach is as accurate in adjudicating AL CA.

Nuclear techniques have emerged as powerful tools in the diagnosis and characterization of CA. It has been recently demonstrated that myocardial uptake of technetium Tc 99m-labeled diphosphonates provides a noninvasive confirmation of ATTR in selected cases (8), whereas it is not useful for the diagnosis of AL, which currently relies on the histological demonstration of amyloid fibrils (9) and requires invasive maneuvers, such as endomyocardial biopsy. Recently, some positron emission tomography (PET)/computed tomography (CT) radiopharmaceuticals developed for the imaging of beta-amyloid deposits within the brain have also shown cardiac uptake, but their usefulness in the diagnostic work-up of patients with CA is still controversial (10–13). Among such radiotracers, fludeoxyglucose F 18 ([18F])-florbetaben, an ^{18}F-labeled stilbene derivative, has a high binding affinity (Ki = 6.7 nmol/l) to brain beta-amyloid (14), whereas there is limited evidence on its application for extracerebral amyloid detection. Two previous studies have reported cardiac [18F]-florbetaben uptake in either AL or ATTR CA by using a static acquisition beginning early after the injection (15 min) and lasting up to 70 min.

We aimed therefore to test the diagnostic value of [18F]-florbetaben PET uptake dynamics for differential diagnosis of cardiac involvement in patients with either AL or ATTR CA.

METHODS

PATIENT POPULATION AND PROTOCOL CRITERIA. Forty patients with biopsy-proven diagnoses of CA (20 ALs and 20 ATTRs) and 20 patients referred to our tertiary center with the initial clinical suspicion of CA and then diagnosed with non-CA conditions were prospectively enrolled and underwent PET/CT with [18F]-florbetaben. Patients <20 years of age and those with coronary artery disease, chronic liver diseases, and severe renal failure (estimated glomerular filtration rate <30 ml/min/1.73 m^2) were excluded. Diagnosis of CA was based on thorough clinical evaluation, biomarkers (N-terminal pro-B-type natriuretic peptide, high-sensitivity troponin T, urine and/or serum immunoglobulin light chains, plasma protein electrophoresis, and serum-free light chains), genetic evaluation for patients with ATTR, electrocardiography, Doppler echocardiography, technetium Tc 99m -hydroxymethylene diphosphonate scintigraphy, cardiac magnetic resonance, and histological evidence of amyloid deposition, according to the most recent indications (8,15). Following the preliminary results from the first 6 patients (AL, ATTR, non-CA; n = 2 each) the sample size was estimated at 9 for each group, given a power of 0.95 and a small effect (G*Power Software, version 3.1, University of Dusseldorf Department of Psychology, Dusseldorf, Germany). On this premise, we have finally enrolled 20 patients in each group. Final diagnosis in the control population included hypertrophic cardiomyopathy in 7 patients, hypertensive heart disease in 10 patients, and dilated cardiomyopathy in 3 patients.

The study protocol conformed to the 1975 Declaration of Helsinki and was approved by the institutional ethics committee and by the Agenzia Italiana del Farmaco committee (EudraCT number: 2017-001660-38); all patients provided written informed consent.

PET/CT IMAGING. All studies were acquired on a Discovery VCT PET/CT scanner (GE Healthcare, Milwaukee, Wisconsin) applying a 3-dimensional

The authors attest they are in compliance with human studies committees and animal welfare regulations of the authors' institutions and Food and Drug Administration guidelines, including patient consent where appropriate. For more information, visit the *JACC: Cardiovascular Imaging* author instructions page.

Manuscript received November 14, 2019; revised manuscript received April 13, 2020, accepted May 4, 2020.

TABLE 1 Clinical, Biohumoral, and Echocardiographic Characteristics of Patients With AL and ATTR Amyloidosis and Those With Non-CA

				p Value			
	AL (n = 20)	ATTR (n = 20)	Non-CA (n = 20)	AL vs. ATTR	AL vs. Non-CA	ATTR vs. Non-CA	Overall
Male	13 (65)	18 (90)	12 (60)	0.031	0.802	0.009	0.002
Age, yes	67.8 ± 9.3	80.7 ± 7.2	71.8 ± 11.6	<0.001	0.120	0.007	<0.001
BMI, kg/m^2	24.4 ± 4.0	25.5 ± 2.9	25.7 ± 2.3	0.261	0.222	0.959	0.389
NYHA functional class I–II/III–IV	7 (36)/13 (64)	14 (70)/6 (30)	15 (75)/5 (25)	0.021	0.021	0.926	0.028
Atrial fibrillation	4 (20)	10 (50)	4 (20)	0.071	0.796	0.045	0.078
Hypertension	8 (40)	10 (50)	9 (45)	0.854	0.565	0.818	0.813
Diabetes	5 (25)	2 (10)	3 (15)	0.204	0.560	0.909	0.191
Hemoglobin, g/dl	12.7 ± 1.6	12.7 ± 1.7	12.2 ± 1.8	0.889	0.535	0.303	0.636
eGFR, ml/min/1.73 m^2	60.8 ± 23.7	62.3 ± 20.9	64.9 ± 30.1	0.955	0.634	0.527	0.815
NT-proBNP, ng/l	5,766 (2,351–13,953)	2,928 (1,677–7,082)	1,013 (494–4,270)	0.235	0.009	0.039	0.17
hs-Troponin T, ng/l	107.5 (48.1–211.3)	60.4 (38.6–115.9)	29.0 (13.3–72.9)	0.373	0.036	0.040	0.048
Beta-blockers	16 (80)	14 (77)	12 (70)	0.562	0.562	0.756	0.526
ACE inhibitors and/or ARBs	11 (55)	14 (70)	11 (55)	0.432	0.851	0.524	0.135
MRA	14 (70)	10 (50)	11 (55)	0.196	0.046	0.927	0.102
LV ejection fraction	52.8 ± 10.2	50.3 ± 11.2	57.5 ± 13.1	0.645	0.136	0.070	0.154
Diastolic dysfunction grade—0/1/2/3	1/3/4/12 (5/15/20/60)	1/3/7/9 (5/15/35/45)	1/10/6/3 (5/50/30/15)	0.654	0.009	0.021	0.020
E/e′	20.8 ± 8.4	20.0 ± 6.2	13.6 ± 5.2	0.596	0.009	0.002	0.005
LA volume index, ml/m^2	22.7 ± 5.0	23.5 ± 4.5	17.6 ± 4.3	0.692	0.004	0.003	0.004
LV end-diastolic volume index, ml/m^2	41.1 ± 8.9	50.3 ± 16.2	63.2 ± 19.2	0.035	<0.001	0.016	0.001
LV end-systolic volume index, ml/m^2	19.2 ± 5.0	25.6 ± 13.3	28.7 ± 17.1	0.129	0.219	0.925	0.270
LV mass indexed, g/m^2	149 ± 39	181 ± 49	129 ± 39	0.044	0.294	0.003	0.009
IVS thickness, mm	16.9 ± 2.8	18.4 ± 3.7	13.1 ± 3.3	0.165	0.001	<0.001	<0.001
Posterior wall thickness, mm	15.2 ± 2.8	16.0 ± 2.9	11.5 ± 2.4	0.329	<0.001	<0.001	<0.001
TAPSE, mm	14.7 ± 3.5	17.6 ± 4.9	19.1 ± 3.2	0.119	0.002	0.341	0.014
PAPs, mm Hg	41 ± 11	43 ± 7	48 ± 22	0.468	0.984	0.310	0.609

Values are n (%), mean ± SD, or median (interquartile range).

ACE = angiotensin-converting enzyme; AL = immunoglobulin light-chain–derived amyloidosis; ARBs = angiotensin receptor blockers; ATTR = transthyretin-related amyloidosis; BMI = body mass index; CA = cardiac amyloidosis; eGFR = estimated glomerular filtration rate (Cockroft-Gault); hs = high-sensitivity; IVS = interventricular septum; LA = left atrial; LV = left ventricular; MRA = mineralocorticoid receptor antagonists; NT-proBNP = N-terminal pro-B-type natriuretic peptide; NYHA = New York Heart Association; PAP = pulmonary artery systolic pressure; TAPSE = tricuspid annular plane systolic excursion.

acquisition protocol. A low-dose CT was first performed through the heart for attenuation correction (effective dose of 1 mSv). All patients then underwent a dynamic cardiac PET/CT scan during the intravenous infusion of 300 MBq/ml of [18F]-Florbetaben followed by a saline flush of 10 ml (1 ml/s); the mean whole-body exposure due to the radiopharmaceutical was 5.8 mSv. Dynamic images were reconstructed from the list-mode scan, performed for up to 60 min. A static cardiac scan (delayed static) was also performed 110 min after [18F]-florbetaben injection.

Images were reviewed on dedicated workstations (Advantage 4.6 and Xeleris 3.1; GE Healthcare). Each static cardiac scan was evaluated visually and reported as "positive" or "negative" considering cardiac visualization, myocardial count uniformity and background noise, especially when lung activity was present. Two experienced nuclear physicians (D.G. and A.G.) performed the qualitative analysis independently, and a consensus was reached on all analyses. Readers were blinded to the patient diagnosis.

Mean standardized uptake value (SUV_{mean}) was defined as the mean voxel intensity within the volumetric region of interest (VOI). The molecular volume (MV) within each VOI was automatically calculated as the sum of all voxels with SUV ≥50% of the SUV_{max} assessed in early images in each single patient. The [18F]-florbetaben cardiac time-activity curve (TAC) was obtained using dynamic reconstructions and by manually drawing a myocardial VOI in the transaxial slice where the left ventricular shape was best represented; plasma TAC was also obtained tracing a circular VOI within the left atrial cavity in the same transaxial slice of the dynamic scan. Moreover, whole-heart static images were retrospectively reconstructed from the dynamic list-mode acquisition between 5 and 15 min (early static), between 30 and 40 min (intermediate static), and between 50 and 60 min (late static). Whole-heart mean SUV (SUV_{mean}), plasma SUV_{mean} (background), and heart-to-background uptake (H/Bkg) ratios were calculated on early, intermediate, and

FIGURE 1 Histological Patterns

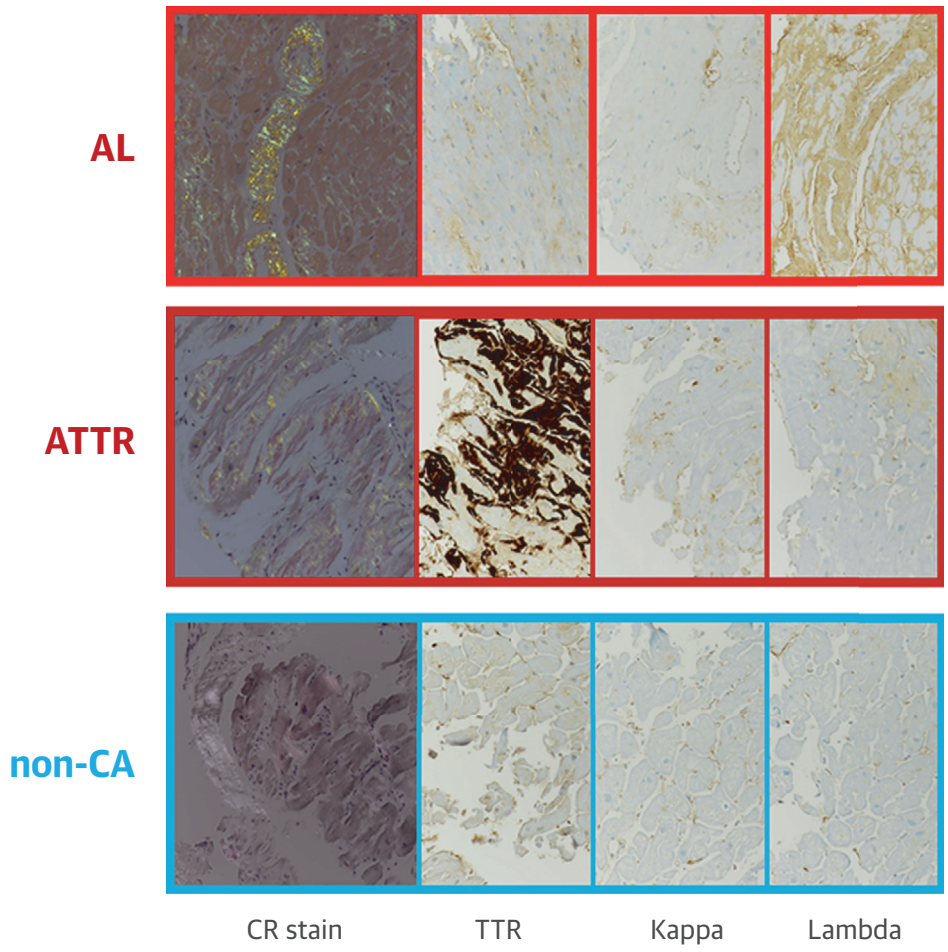

Representative histological patterns from endomyocardial biopsy obtained with Congo-red (CR) staining and immunostaining for transthyretin (TTR), kappa, and lambda immunoglobulin light chains. AL = immunoglobulin light-chain–related amyloidosis; ATTR = transthyretin-related amyloidosis; CA = cardiac amyloidosis.

late scans, as well as on static images obtained at 110 min (delayed). The [18F]-florbetaben myocardial retention index (RI) was calculated as the ratio between the heart SUV_{mean} and the integral of the blood pool TAC in each frame of the dynamic acquisition over a 60-min period after the radiotracer injection according to the formula:

$$\boldsymbol{RI}(\boldsymbol{t}) = TAC_h(t) \Big/ \int_0^t TAC_b(t')dt'$$

where TAC_h = TAC of the heart; TAC_b = TAC of blood pool, t = time, and $'$ = minutes. Further details on PET/CT acquisition and analysis protocol are provided in the Supplemental Methods.

STATISTICAL ANALYSIS. Normal distribution was assessed by the Kolmogorov-Smirnov test; continuous variables with normal distribution were presented as mean ± SD, whereas those with non-normal distribution were presented as median (interquartile range [IQR]); and categorical variables were shown as percentages. Differences among groups were tested by 1-way analysis of variance on ranks (Kruskal-Wallis *H* test) or by chi-square test, as appropriate. A p value of <0.05 was considered significant. Kappa statistics

CENTRAL ILLUSTRATION **Cardiac [18F]-Florbetaben Uptake in Patients With and Without CA**

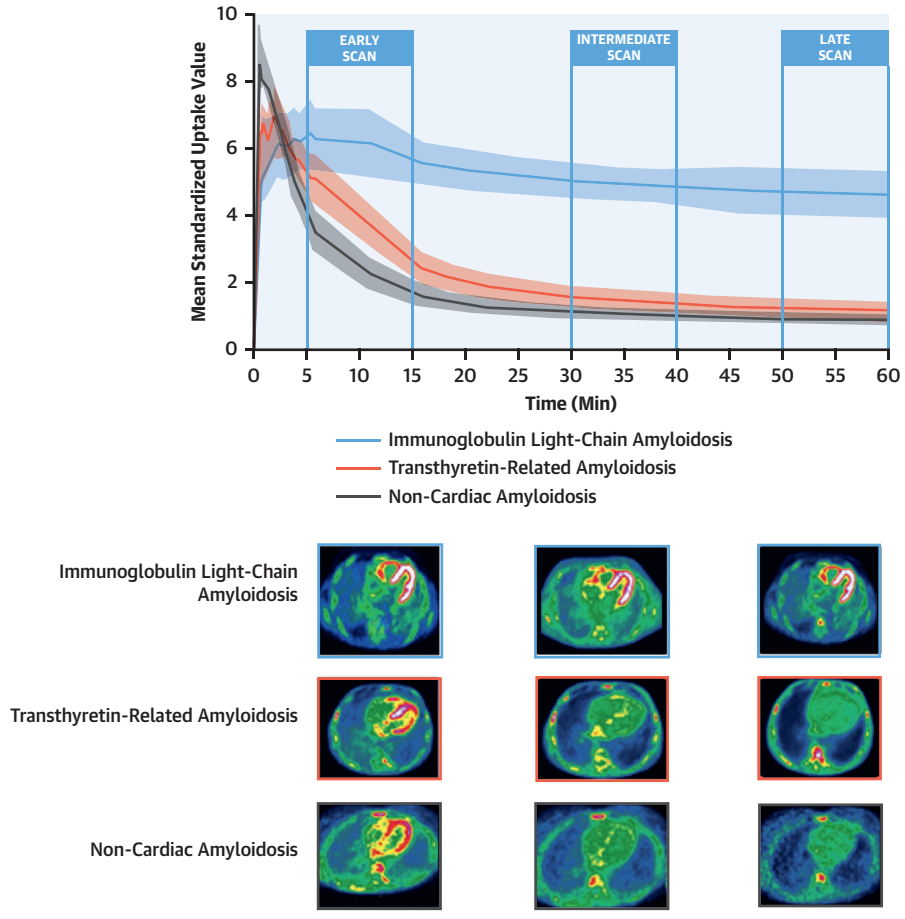

Genovesi, D. et al. J Am Coll Cardiol Img. 2020;■(■):■-■.

(Upper panel) Fludeoxyglucose F 18 ([18F])-florbetaben cardiac positron emission tomography myocardial time-activity curves in patients with immunoglobulin light-chain amyloidosis (AL) **(blue),** transthyretin-related amyloidosis (ATTR) **(red)**, and non-cardiac amyloidosis (non-CA) **(gray)**. The 95% confidence interval is represented as a **shaded area** for each curve. **(Lower panel)** Early (5 to 15 min), intermediate (30 to 40 min), and late (50 to 60 min) [18F]-florbetaben cardiac positron emission tomography scans in patients with AL and ATTR CA and in those with non-CA. SUV_{mean} = mean standardized uptake value.

and SE were calculated to assess the intra- and inter-observer agreement: kappa values <0.4, between 0.4 and 0.75, and >0.75 were taken to represent poor, fair, and good agreement, respectively. Statistical analysis was performed using SPSS version 27 (IBM Corp., Armonk, New York)

RESULTS

CLINICAL CHARACTERISTICS. Clinical characteristics and echocardiographic features of the subjects are summarized in Table 1. Representative histological patterns are shown in Figure 1. Patients with ATTR, compared with those with AL and non-CA, were older and presented with higher left atrial volume and left ventricular mass index (23.5 ± 4.5 ml/m^2; p = 0.003 vs. non-CA; and 129 ± 39 g/m^2; p = 0.003 vs. non-CA, respectively). Furthermore, whereas patients with CA presented with worse diastolic dysfunction, no difference could be observed in terms of left ventricular systolic function when patients with CA were compared with patients with non-CA.

CARDIAC PET/CT CHARACTERISTICS. Static images qualitative analysis. A total of 240 static cardiac scans (4 scans per patient: early; intermediate; late; and delayed) were evaluated by 2 independent observers. Images indicated a significant radiotracer

FIGURE 2 Trend of [18F]-Florbetaben RI for AL, ATTR Amyloidosis and Non-CA Subsets

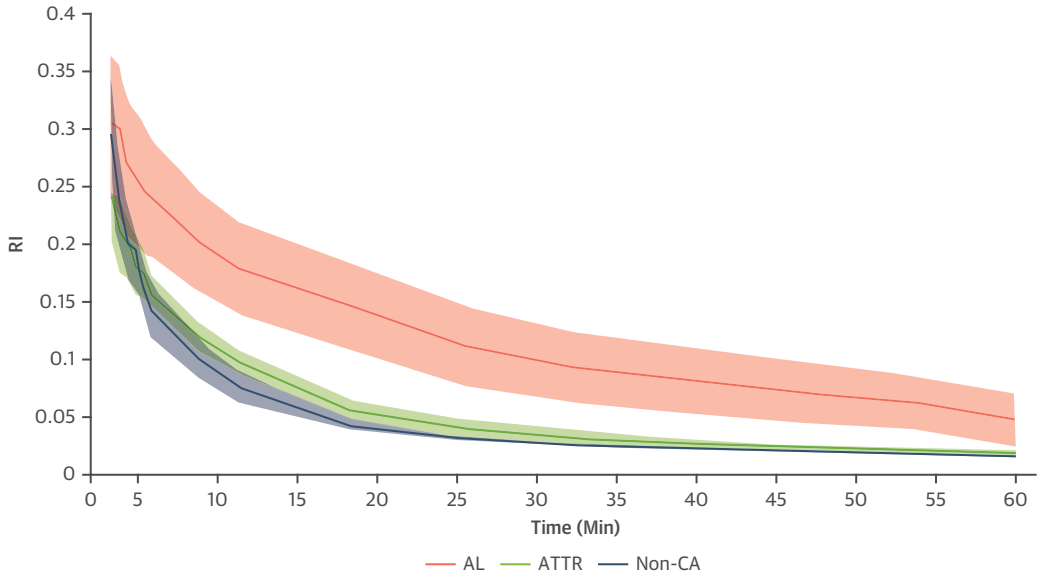

A significant difference in retention index (RI) among patients with AL **(red)** and those with either ATTR **(green)** or non-CA **(blue)** is found within the 20- to 60-min period of observation. No significant difference was found between ATTR and non-CA RI during the whole dynamic acquisition. 18F = fludeoxyglucose F 18; other abbreviations as in Figure 1.

myocardial uptake in 121 of 240 scans (50%) for observer 1 and in 128 of 240 scans (53%) for observer 2; the kappa statistic showed an excellent interobserver ($k = 0.95 \pm 0.02$) and intraobserver ($k = 0.98 \pm 0.02$) agreement.

In the AL group, all ($n = 80$) static images showed significant radiotracer myocardial uptake (100%); in the ATTR group, only 22 of 80 scans (28%) presented myocardial uptake ($n = 20$ early, $n = 2$ intermediate, none among late or delayed scans); in the non-CA group, only the early acquisitions ($n = 16$, 20% of the total) displayed myocardial uptake (**Central Illustration**).

Dynamic quantitative analysis. Mean heart TACs for each group are shown in the **Central Illustration**. In the very early phase (0 to 1.5 min from tracer injection), SUV_{mean} values were significantly greater in patients with non-CA compared with in those with AL and ATTR, whereas it did not differ between patients with AL and those with ATTR. The dynamic phase between 1.5 and 5 min did not show significant differences among groups. From 5 min onward, uptake in patients with AL was greater than that in patients with ATTR and those with non-CA (SUV_{mean}: 5.1; IQR: 4.7 to 5.7; vs. SUV_{mean}: 1.6; IQR: 1.3 to 2.0; and SUV_{mean}: 1.2; IQR: 0.9 to 1.3, respectively; all $p < 0.001$). Within the same time span, uptake in patients with ATTR was also significantly greater than in the patients with non-CA ($p = 0.001$). Mean radiotracer washout between 5 and 60 min evaluated as (SUV_{mean} 5′− SUV_{mean} 60′) / SUV_{mean} 5′ × 100 was significantly lower for patients with AL (22%; 95% confidence interval [CI]: 10% to 34%) than for those with ATTR (74%; 95% CI: 71% to 76%; $p < 0.001$) and those with non-CA (75%; 95% CI: 73% to 77%; $p < 0.001$); no differences were found when comparing patients with ATTR and those with non-CA ($p = 0.678$).

Figure 2 shows the trend of [18F]-florbetaben RI for the AL, ATTR, and non-CA subsets, pointing out that a significant difference in RI between patients with AL (0.091 min^{-1}; IQR: 0.051 to 0.199) and either those with ATTR (0.022 min^{-1}; IQR: 0.019 to 0.028) or non-CA (0.023 min^{-1}; IQR: 0.019 to 0.024; $p < 0.001$ for both comparisons) is found within the 20- to 60-min period of observation. No significant difference was found between ATTR and non-CA RI during the whole dynamic acquisition.

Quantitative images analysis. In the early static reconstructions, cardiac SUV_{mean} was greater in patients with AL than in either patients with ATTR or those with non-CA ($p < 0.001$ for both comparisons), whereas no difference was found between the

TABLE 2 Quantitative PET Parameters of Patients With AL and ATTR Amyloidosis and of Subjects With Non-CA at Early, Intermediate, Late, and Delayed Static Cardiac Scans

				p Value		
	AL (n = 20)	ATTR (n = 20)	Non-CA (n = 20)	AL vs. ATTR	AL vs. Non-CA	ATTR vs. Non-CA
Early Scan (5–15 min)						
SUV_{mean}	5.55 (4.00–7.43)	2.55 (1.80–2.97)	2.50 (1.60–3.37)	<0.001	<0.001	0.960
H/Bkg	4.17 (3.62–6.19)	2.22 (1.79–3.11)	2.11 (1.63–2.77)	0.001	0.002	0.519
MV, ml	208.0 (185.5–290.0)	304.5 (179.0–349.0)	151.0 (100.0–188.1)	0.181	0.002	0.001
Intermediate Scan (30–40 min)						
SUV_{mean}	4.75 (3.70–6.95)	1.45 (1.20–2.10)	1.60 (1.50–1.86)	<0.001	<0.001	0.408
H/Bkg	3.89 (2.73–5.48)	1.58 (1.24–1.82)	1.60 (1.44–1.92)	<0.001	<0.001	0.322
MV, ml	202.0 (166.5–277.5)	96.5 (66.0–167.0)	28.0 (22.0–38.7)	<0.001	<0.001	<0.001
Late Scan (50–60 min)						
SUV_{mean}	4.70 (3.60–6.91)	1.45 (1.15–1.80)	1.60 (1.27–1.87)	<0.001	<0.001	0.552
H/Bkg	4.27 (2.45–5.05)	1.73 (1.30–1.82)	1.55 (1.44–1.80)	<0.001	<0.001	0.987
MV, ml	200.0 (170.0–238.2)	52.0 (39.0–108.0)	14.0 (9.50–16.9)	<0.001	<0.001	<0.001
Delayed (110 min)						
SUV_{mean}	3.50 (2.32–6.10)	1.25 (0.90–1.60)	1.40 (1.20–1.60)	<0.001	<0.001	0.361
H/Bkg	2.51 (2.32–4.49)	1.53 (1.00–1.75)	1.50 (1.32–1.65)	0.001	<0.001	0.608
MV, ml	176.0 (145.0–223.0)	20.5 (7.0–37.0)	7.0 (2.0–12.3)	<0.001	<0.001	0.008

Values are median (interquartile range).

H/Bkg = heart-to-background uptake ratio; MV = molecular volume; PET = positron emission tomography; SUV_{mean} = mean standardized uptake value; other abbreviations as in Table 1.

patients with ATTR and those with non-CA (p = 0.960). With regard to the intermediate static acquisitions, patients with AL had greater cardiac SUV_{mean} than those with ATTR (p < 0.001) and non-CA (p < 0.001), whereas no difference was found between the patients with ATTR and those with non-CA (p = 0.408). The late static acquisitions SUV_{mean} values were greater in patients with AL than in those with ATTR (p < 0.001) and those with non-CA (p < 0.001) and were similar between the patients

FIGURE 3 MVs in Patients With and Without CA

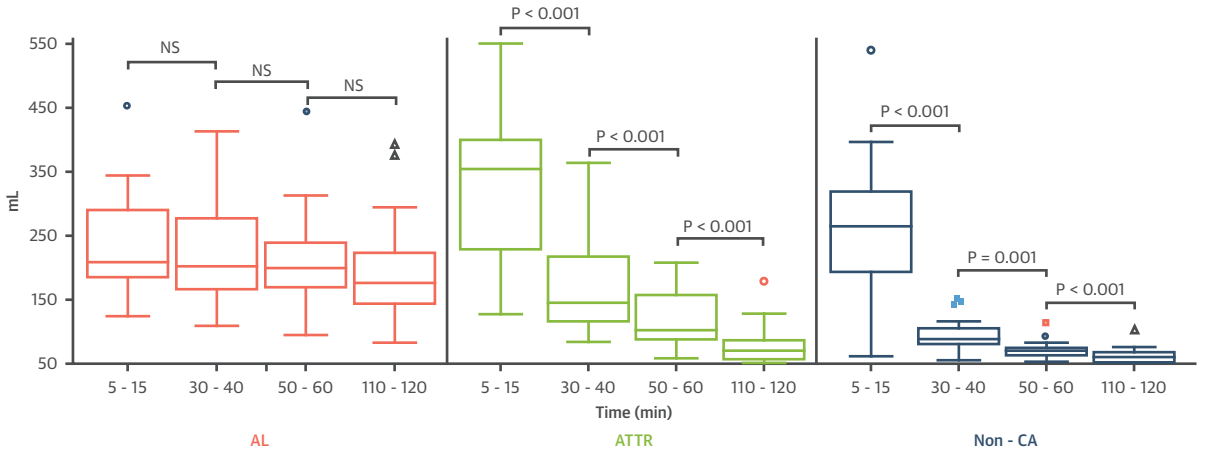

[18F]-florbetaben positron emission tomography molecular volumes (MVs) assessed at different times (5 to 15, 30 to 40, 50 to 60, and 110 to 120 min) after tracer injection in patients with AL and ATTR CA and in patients with non-CA. NS = not significant; other abbreviations as in Figure 1 and 2. The colored symbols refer to the outliers.

with ATTR and those with non-CA ($p = 0.552$). Finally, similar results were obtained at delayed static acquisitions, showing greater SUV_{mean} values in patients with AL compared with those with ATTR ($p < 0.001$) and those with non-CA ($p < 0.001$), whereas no difference was found comparing patients with ATTR and those with non-CA ($p = 0.361$) (**Table 2**). A similar pattern was also observed for H/Bkg ratio, as reported in detail in **Table 2**.

Finally, when comparing MV calculated at 15, 40, 60, and 110 min after radiotracer injection, a progressive decline was found in patients with ATTR and in those with non-CA, whereas it remained stable over time in patients with AL (**Table 2, Figure 3** and Supplemental Figure 1).

Data on SUV_{mean}, H/Bkg ratio, and RI in the 10- to 30-min time frame, which have been object of investigation in previous studies, are reported in Supplemental Table 1, showing significant differences among the AL, ATTR, and non-CA groups.

DISCUSSION

Our results provide the first evidence that late static [18F]-florbetaben PET acquisitions can discriminate cardiac involvement due to AL amyloidosis from ATTR amyloidosis and from other non-CA conditions mimicking infiltrative disorders.

In a previous pilot study, Dorbala et al. (10) showed that an alternative PET radiotracer ([18F]-florbetapir) could differentiate patients affected by either subtype of CA from healthy control subjects ($n = 10$). Nonetheless, in their study, the investigators did not test: 1) in a dedicated analysis; 2) the differences between ATTR or AL; nor 3) extend the uptake analysis beyond 30 min, thus concluding that [18F]-florbetapir could discriminate patients with either amyloidosis subtype from control subjects (who were not indeed selected based on the clinical suspicion of CA) (10). Furthermore, in a paper by Osborne et al. (16), analysis of TACs following [18F]-florbetapir injection, revealed significant differences in estimates of washout rates for patients with CA versus healthy control subjects.

Similar findings were reported in another case-control study, showing that [18F]-florbetaben PET had a significant greater cardiac uptake in patients with either AL or ATTR CA than in control subjects ($n = 5, 5, 4$, respectively). In such study, the investigators dynamically evaluated the cardiac uptake of the radiopharmaceutical performing an 80′ list-mode acquisition and then obtained static images for qualitative and semiquantitative evaluation (11), but they could not report significant differences between patients with ATTR and those with AL. Such inconsistency with our findings may be due to the early analysis by Law et al. (11), who performed a semiquantitative assessment on static images reconstructed between 5 and 10 min after radiotracer injection, well before the time span we have reported to provide discriminating value.

There is recent evidence from a small series of patients with CA that myocardial tracer retention is greater in AL than in ATTR amyloidosis using a 30-min dynamic [18F]-florbetaben-PET/CT acquisition (17), whereas no major difference was reported among disease subtype in terms of visual assessment of cardiac uptake.

The semi-quantitative analysis approach used in this series, performed at different time points up to 110 min after radiotracer injection, allowed us to demonstrate the time-course radiotracer uptake in AL and ATTR CA and in patients presenting with initial clinical suspicion of CA and finally adjudicated to alternative diagnosis. We observed that, whereas early uptake is similar between AL and ATTR amyloidosis, later acquisitions show a significantly greater uptake in patients with AL compared with those with ATTR or without CA. Therefore, a qualitative evaluation of a late scan obtained at least 30 min after radiotracer injection can reliably discriminate cardiac involvement due to AL amyloidosis from ATTR amyloidosis and from non-amyloidotic cardiomyopathy. Also, the greater MV values despite lower left ventricular mass in AL versus ATTR suggests the presence of a type-specific amyloid binding-affinity of [18F]-florbetaben, as further confirmed by the dynamic differences in terms of SUV_{mean} values and H/Bkg ratios. Furthermore, dedicated studies are needed to investigate the molecular mechanisms underlying the differential behavior of the tracer in AL and ATTR amyloidosis.

The time course of myocardial RI indicates that the difference in uptake between AL and both ATTR and non-CA subsets is significant within the 20- to 60-min period after the radiotracer injection, covering the intermediate and late scan periods.

Although serial quantitative analysis performed along the whole acquisition period provides evidence of significant differences between patients with ATTR and nonamyloidotic cardiac involvement in terms of cardiac uptake and of MV, further studies are needed to confirm a possible role of [18F]-florbetaben PET in providing a single test discrimination in patients with suspected CA. Still, our study was underpowered to identify disease-specific diagnostic cutpoints of SUV_{mean} and MV.

We have finally observed a higher amplitude of TAC in the first seconds of myocardial distribution in patients without CA, which is possibly related to better hemodynamics and microvascular function than are found with AL and ATTR.

Our results, when confirmed on a larger basis, may support a central role of [18F]-florbetaben PET imaging in the diagnostic flowchart of patients presenting with suspected CA. Scintigraphy with diphosphonates is currently recommended as a cornerstone examination in patients with suspected CA: intense cardiac uptake without biohumoral evidence of monoclonal component is diagnostic for ATTR, whereas other tests including cardiac magnetic resonance and histological amyloid confirmation are required in patients with no or mild uptake, as well as in patients with monoclonal component. Nonetheless, although an overlap exists in the clinical presentation of AL and ATTR amyloidosis, clinical suspicion is often oriented toward one of either subtype. Although scintigraphy with diphosphonates may be a first-line diagnostic test in subgroups with higher suspicion of TTR-related amyloidosis, [18F]-florbetaben PET could be considered as the first rule-in tool in patients with clinically suspected AL amyloidosis. A timely diagnosis is potentially lifesaving in patients with AL amyloidosis, in particular when cardiac involvement is present, and may hasten the initiation of disease-specific treatment. [18F]-florbetaben PET may represent a single, noninvasive diagnostic tool for AL amyloidosis, thus potentially contributing to improving the time to diagnosis. Moreover, although the mean exposure in our cardiac PET study was lower than the [18F]-florbetaben exposure reported for cerebral scans (see the Supplemental Methods), the use of digital PET/CT scanners may be associated with further reduction of radiation exposure.

STUDY LIMITATIONS. First, we have enrolled a low number of patients. Still, our series is by far the largest studied so far with [18F]-florbetaben PET, and we do provide a thorough clinical, biohumoral, and instrumental characterization of all subjects, including amyloid histological demonstration. As a second point, because none of our patients had mutated ATTR, our results cannot be extended to patients with hereditary forms of ATTR. Finally, a conventional PET/CT scanner was used in our study with a 3-dimensional technology; higher discriminatory performances may be expected from novel digital PET/CT scanners.

CONCLUSIONS

Delayed [18F]-florbetaben cardiac uptake may discriminate CA due to AL from either ATTR or other mimicking conditions. [18F]-florbetaben PET/CT may represent a promising noninvasive first-step tool for the diagnosis of AL amyloidosis, which is still often challenging and delayed.

ADDRESS FOR CORRESPONDENCE: Dr. Michele Emdin, Scuola Superiore Sant'Anna and Fondazione Toscana Gabriele Monasterio, Via Giuseppe Moruzzi 1, 56124 Pisa, Italy. E-mail: emdin@ftgm.it OR m.emdin@santannapisa.it. Twitter: @MicheleEmdin.

PERSPECTIVES

COMPETENCY IN PATIENT CARE AND PROCEDURAL SKILLS: Cardiac involvement from AL amyloidosis holds a poor prognosis and its diagnosis often requires histological demonstration by endomyocardial biopsy. Late [18F]-florbetaben PET/CT scans efficiently discriminate AL CA from ATTR and from other conditions mimicking amyloidosis.

TRANSLATIONAL OUTLOOK: Prospective assessment of the efficacy of [18F]-florbetaben PET/CT in identifying cardiac involvement from AL amyloidosis in a multicenter trial may support its use as a noninvasive diagnostic tool.

REFERENCES

1. Chiti F, Dobson CM. Protein misfolding, functional amyloid, and human disease. Annu Rev Biochem 2006;75:333–66.

2. Falk RH, Comenzo RL, Skinner M. The systemic amyloidoses. N Engl J Med 1997;337:898–909.

3. Westermark P, Bergström J, Solomon A, Murphy C, Sletten K. Transthyretin-derived senile systemic amyloidosis: clinicopathologic and structural consideration. Amyloid 2003;10 Suppl 1:48–54.

4. González-López E, Gallego-Delgado M, Guzzo-Merello G, et al. Wild-type transthyretin amyloidosis as a cause of heart failure with preserved ejection fraction. Eur Heart J 2015;36:2585–94.

5. Mohammed SF, Mirzoyev SA, Edwards WD, et al. Left ventricular amyloid deposition in patients with heart failure and preserved ejection fraction. J Am Coll Cardiol HF 2014;2:113–22.

6. Russo C, Green P, Maurer M. The prognostic significance of central hemodynamics in patients with cardiac amyloidosis. Amyloid 2013;20:199–203.

7. González-López E, López-Sainz Á, Garcia-Pavia P. Diagnosis and treatment of transthyretin cardiac amyloidosis: progress and hope. Rev Esp Cardiol (Engl Ed) 2017;70:991–1004.

8. Gillmore JD, Maurer MS, Falk RH, et al. Nonbiopsy diagnosis of cardiac transthyretin amyloidosis. Circulation 2016;133:2404–12.

9. Bokhari S, Castaño A, Pozniakoff T, Deslisle S, Latif F, Maurer MS. (99m)Tc-pyrophosphate

scintigraphy for differentiating light-chain cardiac amyloidosis from the transthyretin-related familial and senile cardiac amyloidoses. Circ Cardiovasc Imaging 2013;6:195–201.

10. Dorbala S, Vangala D, Semer J, et al. Imaging cardiac amyloidosis: a pilot study using ^{18}F-florbetapir positron emission tomography. Eur J Nucl Med Mol Imaging 2014;41:1652–62.

11. Law WP, Wang WY, Moore PT, Mollee PN, Ng AC. Cardiac amyloid imaging with 18F-florbetaben PET: a pilot study. J Nucl Med 2016;57:1733–9.

12. Lhommel R, Sempoux C, Ivanoiu A, Michaux L, Gerber B. Is 18F-flutemetamol PET/CT able to reveal cardiac amyloidosis? Clin Nucl Med 2014;39:747–9.

13. Genovesi D, Vergaro G, Emdin M, Giorgetti A, Marzullo P. PET-CT evaluation of amyloid systemic involvement with [18F]-florbetaben in patient with proved cardiac amyloidosis: a case report. J Nucl Cardiol 2017;24:2025–9.

14. Zhang W, Oya S, Kung MP, Hou C, Maier DL, Kung HF. F-18 polyethyleneglycol stilbenes as PET imaging agents targeting Aβ aggregates in the brain. Nucl Med Biol 2005;32:799–809.

15. Gillmore JD, Wechalekar A, Bird J, et al. Guidelines on the diagnosis and investigation of AL amyloidosis. Br J Haematol 2015;168:207–18.

16. Osborne DR, Acuff SN, Stuckey A, Wall JS. A routine PET/CT protocol with streamlined calculations for assessing cardiac amyloidosis using (18)F-florbetapir. Front Cardiovasc Med 2015;2:23.

17. Kircher M, Ihne S, Brumberg J, et al. Detection of cardiac amyloidosis with 18F-florbetaben-PET/CT in comparison to echocardiography, cardiac MRI and DPD-scintigraphy. Eur J Nucl Med Mol Imaging 2019;46:1407–16.

KEY WORDS florbetaben, immunoglobulin light-chain–derived amyloidosis, positron emission tomography/computed tomography

APPENDIX For supplemental methods, figure, and table, please see the online version of this paper.